TIPTEKNO'19
TIP TEKNOLOJİLERİ KONGRESİ
MEDICAL TECHNOLOGIES CONGRESS
3-5 Ekim 2019
Kuşadası / Aydın
İZMİR KATİP ÇELEBİ ÜNİVERSİTESİ

Simultaneus Estimation and Control of Glucose-Insulin Dynamics in Type-1 Diabetes

Meric Cetin
Dept. of Computer Eng.
Pamukkale University
Denizli, Turkey
mcetin@pau.edu.tr

Selami Beyhan
Dept. of Electrical and Electronics Eng.
Izmir Democracy University
Izmir, Turkey
selami.beyhan@idu.edu.tr

***Abstract*—This paper proposes an observer-controller configuration for the well-known Hovarka Glucose-Insulin dynamics. The aim is to control the blood glucose level without measuring the states in the Hovarka model. In order that nonlinear model predictive control is designed to control the blood glucose level by considering the random inertial glucose inputs under external insulin inputs. For the estimation, a Cubature Kalman filter is designed to estimate the states. Numerical computations are conducted under random glucose inputs from the meals where the applied observer-controller configuration provides blood glucose control without measuring the states. As a result, by using a single subcutaneous glucose measurement, the Hovarka glucose-insuling dynamics can be controlled for a possible portable device in future.**

Keywords*—Type-1 diabetes, cubature Kalman filter,model predictive control.

I. Introduction

The insulin required to regulate blood glucose levels (BGL) in type 1 diabetes mellitus (T1DM), which is a chronic autoimmune disease affecting the pancreas, cannot be produced. In medical treatment, insulin injection is required to maintain BGL within the desired range. However, it is very difficult to maintain blood glucose concentration within the target range [1]. Many factors, such as type of food, exercise or stress, are associated with insulin-BGL interaction. Exceeding the maximum and minimum target ranges (hyperglycemia/hypoglycemia) causes health complications such as cardiovascular disease, organ failure, blindness, coma and death [2].

The automated insulin delivery system, known as the artificial pancreas (AP), is a control mechanism that provides the loop between glucose-sensing and insulin-delivery [3]. In the literature, various control algorithms such as proportional integral derivative control (PID) [4], fuzzy logic control [5], model predictive control (MPC) [6] have been proposed based on commonly used models (Bergman model [7], Hovorka model [6] and Dalla Man model [8]) for AP systems. Accurate estimation of high variability of insulin level is important to limit insulin delivery in the patient. It is possible to analyze the effect of this variability with a observer based model predictive controller design.

978-1-7281-2420-9/19/$31.00 ©2019 IEEE

In this paper, the state estimation of the Hovarka glucose-insulin dynamics are achieved using fast and accurate observer design. The observer is designed based on the system dynamics and second-order gradient update. The main goal of the paper is to estimate instantaneous variables of the glucose and insulin. The most important parameter for the T1DM is the simulataneous carbohydrate intake. Its amount and concentration for the blood is unexpectable and difficult for the human health. The designed observer-controller estimates the unmeasured blood glucose dynamics and stabilizes plasma glucose level under the disturbance of random glucose inputs from the meals.

II. The Glucose Insulin Dynamic Model of Hovorka

The glucose-insulin dynamic model of Hovorka, which characterizes blood glucose dynamics, subcutaneous insulin infusion and transport of glucose from plasma to tissues, is given as [6]:

$$\begin{aligned}
\dot{S}_1(t) =& u(t) - \frac{S_1(t)}{t_{max,l}(t)},\\
\dot{S}_2(t) =& \frac{S_1(t)}{t_{max,l}(t)} - \frac{S_2(t)}{t_{max,l}(t)},\\
\dot{I}(t) =& \frac{S_2(t)}{t_{max,l}(t)V_I} - k_e(t)I(t),\\
\dot{x}_1(t) =& -k_{a1}x_1(t) + I(t)(S^f_{IT} \times k_{a1}),\\
\dot{x}_2(t) =& -k_{a2}x_2(t) + I(t)(S^f_{ID} \times k_{a2}),\\
\dot{x}_3(t) =& -k_{a3}x_3(t) + I(t)(S^f_{IE} \times k_{a3}),\\
\dot{Q}_1(t) =& U_G(t) - F^c_{01}(t) - F_R(t) - x_1(t)Q_1(t)\\
&+ k_{12}Q_2(t) + EGP_0(1 - x_3(t)),\\
\dot{Q}_2(t) =& x_1(t)Q_1(t) - (k_{12} + x_2(t))Q_2(t),\\
\dot{G}_{sub}(t) =& \frac{1}{\tau}(\frac{Q_1(t)}{V_G} - G_{sub}(t)).
\end{aligned} \tag{1}$$

where

$$F^c_{01} = \begin{cases} F_{01} & \text{if } G_{sub}(t) \geq 4.5 \text{ mmol/L} \\ F_{01}G_{sub}(t)/4.5 & \text{otherwise} \end{cases} \tag{2}$$

$$F_R = \begin{cases} 0.003(G_{sub}(t) - 9)V_G & \text{if } G_{sub}(t) \geq 9 \text{ mmol/L} \\ 0 & \text{otherwise} \end{cases} \tag{3}$$

TABLE I. PARAMETERS OF THE T1DMS MODEL [8].

Symbol	Definition/Value(unit)
$S_1(t)$	Subcutaneously administered insulin absorption (mU)
$S_2(t)$	Subcutaneously administered insulin absorption (mU)
$I(t)$	Plasma insulin concentration (mUL^{-1})
$x_1(t)$	Effects of insulin on glucose distribution/transport (min^{-1})
$x_2(t)$	Effects of insulin on glucose disposal (min^{-1})
$x_3(t)$	Effects of insulin on endogenous glucose production (min^{-1})
$Q_1(t)$	Masses of glucose in the accessible compartment (mmol)
$Q_2(t)$	Masses of glucose in the non-accessible compartment (mmol)
$G_{sub}(t)$	Subcutaneous glucose (mmolL^{-1})
$U_G(t)$	Gut absorption rate (mmolmin^{-1})
$u(t)$	Administration (bolus and basal) of insulin (mUmin^{-1})
BW	Weight (kg)
k_e	Insulin elimination from plasma (0.138 min^{-1})
$t_{max,I}$	Time-to-maximum of absorption of injected insulin (55 min)
$t_{max,G}$	Time-of-maximum appearance rate of glucose (40 min)
k_{12}	Transfer rate (0.066 min^{-1})
k_{a1}	Deactivation rate (0.006 min^{-1})
k_{a2}	Deactivation rate (0.06 min^{-1})
k_{a3}	Deactivation rate (0.03 min^{-1})
V_I	Insulin distribution volume (0.12×BWL)
V_G	Glucose distribution volume (0.16×BWL)
S_{IT}^f	Insulin sensitivity of distribution/transport (51.2×10^{-4}Lmin^{-1}mU^{-1})
S_{ID}^f	Insulin sensitivity of disposal (8.2×10^{-4}Lmin^{-1}mU^{-1})
S_{IE}^f	Insulin sensitivity of EGP (520×10^{-4}LmU^{-1})
EGP_0	EGP extrapolated to zero insulin concentration (0.0161mmolkg^{-1}min^{-1})
F_{01}	Non-insulin-dependent glucose flux (0.0097mmolkg^{-1}min^{-1})

In Hovarka's model, the gut absorption rate is given as

$$U_G(t) = \frac{D_G A_G t e^{-t/t_{max,G}}}{t_{max,G}^2} \tag{4}$$

where D_G is the estimated carbohydrate intake [mmol/kg] and A_G is the carbohydrate bioavailability [unitless]. The injected insulin (basal and bolus) ($u(t)$) is the input signal and the subcutaneous glucose concentration ($G_{sub}(t)$) is the output signal of the glucose-insulin dynamic model. The all variables and parameters of the Hovarka's model are given in Table I.

III. CUBATURE KALMAN TYPE FILTERING BASED PREDICTIVE CONTROL

To apply a cubature Kalman filter based model predictive controller, consider a nonlinear discrete-time system in state-space representation as

$$\begin{aligned} \mathbf{x}_{k+1} &= \hat{\mathbf{f}}(\mathbf{x}_k, \mathbf{u}_k) + \boldsymbol{w}_k, \\ \mathbf{y}_k &= \hat{\mathbf{h}}(\mathbf{x}_k, \mathbf{u}_k) + \mathbf{v}_k \end{aligned} \tag{5}$$

where $\mathbf{x}_k \in \Re^N$, $\mathbf{u}_k \in \Re^{R_u}$ and $\mathbf{y}_k \in \Re^{Q_y}$ represent the state vector, the control signal and the measurement output signal, respectively. $\boldsymbol{w}_k \sim N(\mathbf{0}, \mathbf{Q}_k)$ is the Gaussian process noise and $\mathbf{v}_k \sim N(\mathbf{0}, \mathbf{R}_k)$ is the Gaussian measurement noise. It is assumed that the system (5) is controllable and observable. The nonlinear functions $\hat{\mathbf{f}}(.)$ and $\hat{\mathbf{h}}(.)$ are known discretized and differentiable functions with respect to the states and control signal of the nonlinear system.

A. Cubature Kalman Filter

General estimation applications for CKF are performed using a series of cubature points [9]. The augmented vectors containing the unmeasurable states and covariance matrix for CKF are expressed as

$$\mathbf{x}_k^{aug} = [\mathbf{x}_k^T \quad \boldsymbol{w}_k^T \quad \mathbf{v}_k^T], \quad \mathbf{P}_k^{aug} = \begin{bmatrix} \mathbf{P}_k^x & 0 & 0 \\ 0 & \mathbf{Q}_k & 0 \\ 0 & 0 & \boldsymbol{R}_k \end{bmatrix} \tag{6}$$

where $\mathbf{P}_k^x$ is the state error covariance matrix. The cubature Kalman filter that performs the estimation process includes the following steps.

1) **Filter initialization**
$\hat{\mathbf{x}}_{0|0} = E[\mathbf{x}_0], \mathbf{P}_{0|0} = E[(\mathbf{x}_0 - \hat{\mathbf{x}}_0)(\mathbf{x}_0 - \hat{\mathbf{x}}_0)^T]$
Generate the cubature points $\xi_i = \sqrt{n_x}\{1\}_i$ and $\{1\}_i$ is the ith point of

$$\{1\} = \left\{ \begin{pmatrix} 1 \\ 0 \\ \vdots \\ 0 \end{pmatrix}, \ldots, \begin{pmatrix} 0 \\ \vdots \\ 0 \\ 1 \end{pmatrix}, \begin{pmatrix} -1 \\ 0 \\ \vdots \\ 0 \end{pmatrix}, \ldots, \begin{pmatrix} 0 \\ \vdots \\ 0 \\ -1 \end{pmatrix} \right\}.$$

Generate the weights: $w_i = w = \frac{1}{2n_x}$

2) **Time update equations (Prediction)**
Perform Cholesky decomposition for $\mathbf{P}_{k|k} = C_{k|k} C_{k|k}^T$ and propagate cubature points:
$\boldsymbol{\chi}_{i,k|k} = \sqrt{n_x} C_{k|k} \xi_i + \hat{\mathbf{x}}_{k|k}$
$\boldsymbol{\chi}_{i,k+1|k} = \hat{\mathbf{f}}(\boldsymbol{\chi}_{i,k|k}, \hat{\boldsymbol{\theta}}_k, \mathbf{u}_k)$. These points are used to set covariance matrix and estimated output value. Compute the propagated state and covariance matrix:
$\hat{\mathbf{x}}_{k+1|k} = w \sum_{i=1}^{2n_x} \boldsymbol{\chi}_{i,k+1|k}$
$\mathbf{P}_{k+1|k} = w \sum_{i=1}^{2n_x} (\boldsymbol{\chi}_{i,k+1|k} - \hat{\mathbf{x}}_{k+1|k})(\boldsymbol{\chi}_{i,k+1|k} - \hat{\mathbf{x}}_{k+1|k})^T + \mathbf{Q}_k$.

3) **Measurement update equations (Update)**
Define the error covariance matrix with $\zeta > 0$ as $\mathbf{P}^* = (\mathbf{P}_{k+1|k}^{-1} - \zeta \mathbf{I})^{-1}$, such that $\mathbf{P}^* > 0$.
Perform Cholesky decomposition for $\mathbf{P}^* = (C_{k+1|k} C_{k+1|k}^T)$. Propagate new cubature points throught the measurement process:
$\boldsymbol{\chi}_{i,k+1|k} = \sqrt{n_x} C_{k+1|k} \xi_i + \hat{\mathbf{x}}_{k+1|k}$
$\boldsymbol{\eta}_{i,k+1|k} = \hat{\mathbf{h}}(\boldsymbol{\chi}_{i,k+1|k}, \hat{\boldsymbol{\theta}}_k, \mathbf{u}_k)$.
Calculate the estimated measurement, innovation covariance and cross covariance matrix:
$\hat{\mathbf{y}}_{k+1|k} = w \sum_{i=1}^{2n_x} \boldsymbol{\eta}_{i,k+1|k}$
$\mathbf{P}_{y|k+1} = w \sum_{i=1}^{2n_x} (\boldsymbol{\eta}_{i,k+1|k} - \hat{\mathbf{y}}_{k+1|k})(\boldsymbol{\eta}_{i,k+1|k} - \hat{\mathbf{y}}_{k+1|k})^T + \mathbf{R}_k$
$\mathbf{P}_{xy|k+1} = w \sum_{i=1}^{2n_x} (\boldsymbol{\chi}_{i,k+1|k} - \hat{\mathbf{x}}_{k+1|k})(\boldsymbol{\eta}_{i,k+1|k} - \hat{\mathbf{y}}_{k+1|k})^T$
Compute the Kalman gain for state estimation, update state and covariance matrix:
$\mathbf{K}_{k+1} = \mathbf{P}_{xy|k+1} \mathbf{P}_{y|k+1}^{-1}$
$\hat{\mathbf{x}}_{k+1|k+1} = \hat{\mathbf{x}}_{k+1|k} + \mathbf{K}_{k+1}(\mathbf{y}_{k+1} - \hat{\mathbf{y}}_{k+1})$
$\mathbf{P}_{k+1|k+1} = \mathbf{P}_{k+1|k} + \mathbf{K}_{k+1} \mathbf{P}_{y|k+1} \mathbf{K}_{k+1}^T$

This algorithm represents the fundamental CKF state estimation process. The resulting cubature points provide robust and risk-sensitive filter design [10].

B. Nonlinear Model Predictive Control

A nonlinear model predictive controller (NMPC) can be designed for given system in Eq.(5). The discrete-time NMPC

structure is expressed as a constrained optimization problem:

$$\begin{aligned}
&\min_{\mathbf{u}} F(x_k, u_k), \quad \text{subject to} \\
&\mathrm{X}_i = \{x_i \in \Re \mid \quad x_{i_{min}} \le x_i \le x_{i_{max}}, i = 1, \ldots, n_x\} \\
&\mathrm{U}_r = \{u_r \in \Re \mid \quad u_{r_{min}} \le u_r \le u_{r_{max}}, r = 1, \ldots, n_u\} \\
&\Delta\mathrm{U}_r = \{\Delta u_r \in \Re \mid \quad |\Delta u_r| \le \Delta u_{r_{max}}, r = 1, \ldots, n_{ud}\} \\
&\mathrm{Y}_q = \{y_q \in \Re \mid \quad y_{q_{min}} \le y_q \le y_{q_{max}}, q = 1, \ldots, n_y\}
\end{aligned} \tag{7}$$

with

$$F(u_k) = \frac{1}{2}\sum_{p=1}^{\kappa}\sum_{j=1}^{n_y}(\tilde{y}_{j|k+p} - \hat{y}_{j|k+p})^2 + \frac{1}{2}\lambda_r\sum_{r=1}^{n_{ud}}(u_{r|k+1} - u_{r|k})^2 \tag{8}$$

where $\Delta\mathrm{U}_r$ is the input/input slew constraints, λ_r is the penalty term for input signal and κ is the prediction horizon, respectively. In (8), $\hat{y}_{q|k+\kappa}$ is the estimation value for the *qth* output and $\tilde{\mathbf{y}}$ is the reference signal vector whose short-term future values are known. The minimization of constrained optimization problem in (8) is performed by nonlinear optimization algorithm (Levenberg-Marquardt) in the nonlinear MPC structure [11]. The aim in NMPC structure is to calculate the optimal signal that will lead the system to desired trajectory. When the first component of $\mathbf{u}_{k+1} = [u_{1|k}, \ldots, u_{r|k}]^{\mathrm{T}}$ is applied to the system as much as κ-times, predictions are generated. By using future predictions, when $F(\mathbf{u}_{k+1} + \delta\mathbf{u}_{k+1}) < F(\mathbf{u}_{k+1})$ is achived, optimal control signal is updated by adding a correction term ($\delta\mathbf{u}_{k+1}$). The update rule for $\mathbf{u}_{k+1}$ is written as

$$\mathbf{u}_{k+1} \Longleftarrow \mathbf{u}_k + \delta\mathbf{u}_{k+1}, \tag{9}$$

$$\delta\mathbf{u}_{k+1} = -(\mathbf{J}_u^T\mathbf{J}_u + \mu_u\mathbf{I})^{-1}\mathbf{J}_u^T\hat{\mathbf{e}}, \tag{10}$$

where $\hat{\mathbf{e}}$ is the prediction error vector

$$\hat{\mathbf{e}} = \begin{bmatrix} \tilde{y}_{1|k+1} - \hat{y}_{1|k+1} \\ \vdots \\ \tilde{y}_{q|k+\kappa} - \hat{y}_{q|k+\kappa} \\ \sqrt{\lambda_1}\Delta\mathbf{u}_{k+1} \\ \vdots \\ \sqrt{\lambda_{\mathrm{R}}}\Delta\mathbf{u}_{k+1} \end{bmatrix}, \tag{11}$$

and

$$\mathbf{J}_u = -\begin{bmatrix} \frac{\partial\hat{y}_{1|k+1}}{\partial u_{1|k+1}} & \frac{\partial\hat{y}_{1|k+1}}{\partial u_{2|k+1}} & \cdots & \frac{\partial\hat{y}_{1|k+1}}{\partial u_{r|k+1}} \\ & & \vdots & \\ \frac{\partial\hat{y}_{q|k+\kappa}}{\partial u_{1|k+1}} & \frac{\partial\hat{y}_{q|k+\kappa}}{\partial u_{2|k+1}} & \cdots & \frac{\partial\hat{y}_{q|k+\kappa}}{\partial u_{r|k+1}} \\ \sqrt{\lambda_1} & \sqrt{\lambda_1} & \cdots & \sqrt{\lambda_1} \\ \sqrt{\lambda_{\mathrm{R}}} & \sqrt{\lambda_{\mathrm{R}}} & \cdots & \sqrt{\lambda_{\mathrm{R}}} \end{bmatrix}. \tag{12}$$

Each term ($\frac{\partial\hat{y}_{q|k+\kappa}}{\partial u_{r|k+1}}$) in $\mathbf{J}_u$ matrix is derived from the sampled nonlinear system model [12].

IV. Computational Results

The numerical computations are presented to show the applicability of the designed observer-controller configuration. The sampling time is selected as $T_s = 5$ minute. By the grid search of a reasonable interval, the controller and observer parameters are selected. The controller parameters are as follows: $\kappa = 20, \Delta\mathrm{U}_r = 1, \lambda_r = 10^{-4}$. In addition, the selected observer parameters are as follows: $\mathbf{P} = 10^{-6}\mathbf{I}_{n\times n}, \mathbf{Q} = 10^{-7}\mathbf{I}_{n\times n}, R = 10^6$. In Figure 1, the stabilization of the blood glucose is shown where the applied external input is given in Figure 2. Figure 3 and Figure 4 show the state estimation results of the glucose-insulin dynamic model under random glucose input.

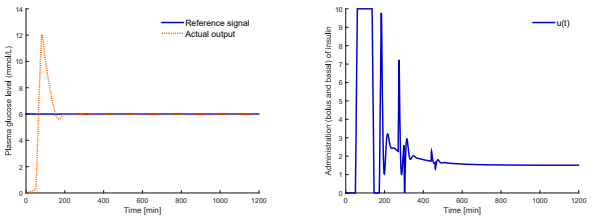

(a) Plasma glucose control $G_{sub}(t)$. (b) Applied insulin level.

Fig. 1. Stabilization results.

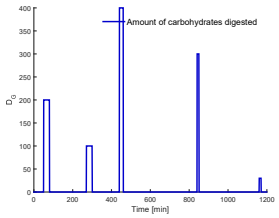

Fig. 2. External input.

V. Conclusion

Sensorless control of the glucose dynamics is performed using cubature Kalman filter-nonlinear model predictive control configuration in this paper. Unmeasured states are estimated by the designed cubature Kalman filter. By using estimated dynamics, the blood glucose dynamics are controlled by an external insulin input under the disturbance of random glucose inputs from the meals. The designed controller provided applicable simulation results for a possible glucose controller device in future.

Acknowledgment

This paper is supported by Pamukkale University Scientific Research Projects Council under grand number 2019KRM004-059.

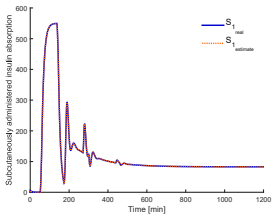

(a) $S_1(t)$

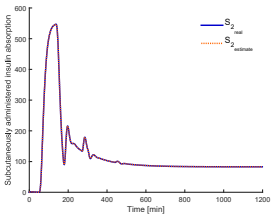

(b) $S_2(t)$

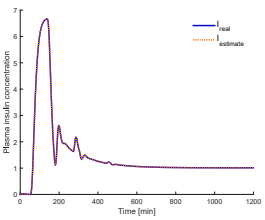

(c) $I(t)$

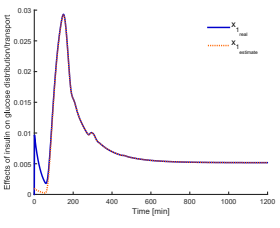

(d) $x_1(t)$

Fig. 3. State estimation results-1.

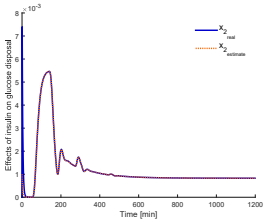

(a) $x_2(t)$

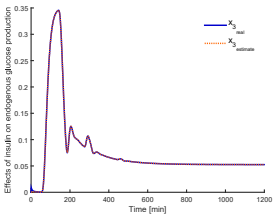

(b) $x_3(t)$

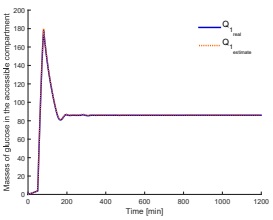

(c) $Q_1(t)$

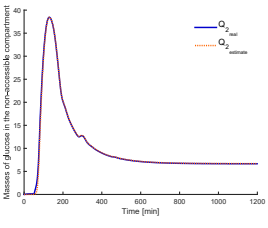

(d) $Q_2(t)$

Fig. 4. State estimation results-2.

REFERENCES

[1] G. C. Goodwin and M. M. Seron, "Feedback and feedforward control in the context of model predictive control with application to the management of type 1 diabetes mellitus," *Control Engineering Practice*, vol. 89, pp. 228–237, 2019.

[2] S. L. Aronoff, K. Berkowitz, B. Shreiner, and L. Want, "Glucose metabolism and regulation: beyond insulin and glucagon," *Diabetes spectrum*, vol. 17, no. 3, pp. 183–190, 2004.

[3] I. Hajizadeh, M. Rashid, and A. Cinar, "Plasma-insulin-cognizant adaptive model predictive control for artificial pancreas systems," *Journal of Process Control*, vol. 77, pp. 97–113, 2019.

[4] G. Marchetti, M. Barolo, L. Jovanovic, H. Zisser, and D. E. Seborg, "An improved pid switching control strategy for type 1 diabetes," *ieee transactions on biomedical engineering*, vol. 55, no. 3, pp. 857–865, 2008.

[5] R. Mauseth, I. B. Hirsch, J. Bollyky, R. Kircher, D. Matheson, S. Sanda, and C. Greenbaum, "Use of a fuzzy logic controller in a closed-loop artificial pancreas," *Diabetes technology & therapeutics*, vol. 15, no. 8, pp. 628–633, 2013.

[6] R. Hovorka, V. Canonico, L. J. Chassin, U. Haueter, M. Massi-Benedetti, M. O. Federici, T. R. Pieber, H. C. Schaller, L. Schaupp, T. Vering, *et al.*, "Nonlinear model predictive control of glucose concentration in subjects with type 1 diabetes," *Physiological measurement*, vol. 25, no. 4, p. 905, 2004.

[7] R. N. Bergman, L. S. Phillips, and C. Cobelli, "Physiologic evaluation of factors controlling glucose tolerance in man: measurement of insulin sensitivity and beta-cell glucose sensitivity from the response to intravenous glucose." *The Journal of clinical investigation*, vol. 68, no. 6, pp. 1456–1467, 1981.

[8] C. Dalla Man, R. A. Rizza, and C. Cobelli, "Meal simulation model of the glucose-insulin system," *IEEE Transactions on biomedical engineering*, vol. 54, no. 10, pp. 1740–1749, 2007.

[9] I. Arasaratnam and S. Haykin, "Cubature kalman filters," *IEEE Transactions on automatic control*, vol. 54, no. 6, pp. 1254–1269, 2009.

[10] I. Arasaratnam, S. Haykin, and T. R. Hurd, "Cubature kalman filtering for continuous-discrete systems: theory and simulations," *IEEE Transactions on Signal Processing*, vol. 58, no. 10, pp. 4977–4993, 2010.

[11] E. F. Camacho and C. B. Alba, *Model predictive control*. Springer Science & Business Media, 2013.

[12] S. Iplikci, "Rungekutta model-based adaptive predictive control mechanism for non-linear processes," *Transactions of the Institute of Measurement and Control*, vol. 35, no. 2, pp. 166–180, 2013.